Received: 8 September 2022 | Revised: 19 December 2022 | Accepted: 27 December 2022

DOI: 10.1111/pce.14528

ORIGINAL ARTICLE

Plant, Cell & Environment | WILEY

Inactivation of RPX1 in *Arabidopsis* confers resistance to *Plutella xylostella* through the accumulation of the homoterpene DMNT

Hongyi Chen[1] | Chen Chen[1,2] | Shijie Huang[1] | Mengjie Zhao[1] | Tengyue Wang[1] | Taoshan Jiang[1] | Chuanhong Wang[1] | Zhen Tao[1] | Yan Zhang[1] | Yunhe Wang[1] | Wanyi Wang[1] | Qingfeng Tang[3] | Peijin Li[1]

[1]The National Engineering Lab of Crop Stress Resistance Breeding, School of Life Sciences, Anhui Agricultural University, Hefei, China

[2]Department of Microbiology, the Key Laboratory of Microbiology and Parasitology of Anhui Province, the Key Laboratory of Zoonoses of High Institutions in Anhui, School of Basic Medical Sciences, Anhui Medical University, Hefei, China

[3]Key Laboratory of Biology and Sustainable Management of Plant Diseases and Pests of Anhui Higher Education Institutes, School of Plant Protection, Anhui Agricultural University, Hefei, China

Correspondence
Peijin Li, The National Engineering Lab of Crop Stress Resistance Breeding, School of Life Sciences, Anhui Agricultural University, Hefei 230036, China.
Email: Peijin.li@ahau.edu.cn

Funding information
Anhui Provincial Major Science and Technology Project; National Natural Science Foundation of China

Abstract

The lepidopteran crop pest *Plutella xylostella* causes severe constraints on *Brassica* cultivation. Here, we report a novel role for *RPX1* (resistance *to P. xylostella*) in resistance to this pest in *Arabidopsis thaliana*. The *rpx1-1* mutant repels *P. xylostella* larvae, and feeding on the *rpx1-1* mutant severely damages the peritrophic matrix structure in the midgut of the larvae, thereby negatively affecting larval growth and pupation. This resistance results from the accumulation of defence compounds, including the homoterpene (3*E*)−4,8-dimethyl-1,3,7-nonatriene (DMNT), due to the upregulation of *PENTACYCLIC TRITERPENE SYNTHASE 1* (*PEN1*), which encodes a key DMNT biosynthetic enzyme. *P. xylostella* infestation and wounding induce RPX1 protein degradation, which may confer a rapid response to insect infestation. *RPX1* inactivation and *PEN1* overexpression are not associated with negative trade-offs for plant growth but have much higher seed production than the wild-type in the presence of *P. xylostella* infestation. This study offers a new strategy for plant molecular breeding against *P. xylostella*.

KEYWORDS
pest resistance, secondary metabolism, volatile emissions

1 | INTRODUCTION

Insect pests not only reduce crop yield but also affect the quality of crop products (Johnson & Züst, 2018; Wu et al., 2016; Zhao et al., 2016). Among them, the diamondback moth *Plutella xylostella* is a widely distributed and harmful lepidopteran pest that feeds on cruciferous crops such as cauliflower and cabbage, causing tremendous economic losses. Currently, in agricultural management, pest control using agrochemicals (e.g., pesticides) has been very successful and heavily applied, but this approach is becoming problematic owing to potential environmental contamination and threats to human health (Shakeel et al., 2017). An alternative approach to crop production is the use of genetically engineered crops with enhanced resistance to pests, for example in planta

Hongyi Chen, Chen Chen, Shijie Huang and Mengjie Zhao have equal contribution to this work.

expression of *Bacillus thuringiensis* (Jouzani et al., 2017) or other heterologous entomotoxic proteins (Douglas, 2018). Extensive efforts have been made to identify new approaches to control *P. xylostella* in agriculture; however, effective genes, natural pesticides and resistant germplasm remain limited (Zhou & Jander, 2021).

Through a constant arms race with insect pests, plants have evolved various abilities to combat insect attacks. Accordingly, plants synthesise arrays of defensive metabolites such as benzoxazinoids (Handrick et al., 2016; Varsani et al., 2019), methyl benzoate (Feng & Zhang, 2017) and serotonin (Lu et al., 2018) in response to pest injury. Jasmonic acid (JA), also called 'wound hormone', plays a central role in various wound-related damage responses initiated by insect infestation (Lortzing & Steppuhn, 2016). Increasing evidence suggests that JA functions synergistically and/or antagonistically with other phytohormones, such as salicylic acid (SA) and ethylene (Costarelli et al., 2020; Ma et al., 2019). In addition to direct defences, plants damaged by insect attacks release various volatile compounds that attract the natural enemies of herbivores (Gols, 2014). Of these complex volatile blends, the homoterpene compounds (3*E*)−4,8-dimethyl-1,3,7-nonatriene (DMNT) and (*E*,*E*)−4,8,12-trimethyl-1,3,7,11-tridecatetraene (TMTT) have been reported in multiple plant species such as *Arabidopsis* (Lee et al., 2010; Sohrabi et al., 2015), rice (Li et al., 2018), maize (Gouinguené et al., 2005; Richter et al., 2016) and cotton (Liu et al., 2018). Several studies have also indicated that DMNT acts as a signal molecule that induces anti-herbivore defences during plant-plant communication (Arimura et al., 2000; Meents et al., 2019). For instance, after incurring damage from chewing insects, some sweet potatoes emit DMNT, which results in the systemic induction of the protease inhibitor sporamin in neighbouring sweet potato plants and makes them indigestible to insects (Meents et al., 2019). Similar results have been observed for tea plants (Jing et al., 2020). Recently, we found that DMNT plays a role in killing *P. xylostella* larvae by disrupting the peritrophic matrix (PM) barrier in the insect midgut (Chen et al., 2021).

In higher plants, the DMNT and TMTT biosynthesis pathways have been well-characterised through reverse genetics and biochemical analyses. In maize, DMNT and TMTT are produced from the oxidative degradation of (E)-nerolidol and (E,E)-geranyllinalool by two P450 monooxygenases, CYP92C5 and CYP92C6 (Richter et al., 2016). In cotton, two CYP genes (*GhCYP82L1* and *GhCYP82L2*) are responsible for the conversion of (E)-nerolidol into DMNT and (E,E)-geranyllinalool into TMTT (Liu et al., 2018). In *Arabidopsis* roots, DMNT is catalysed from the precursor C_{30} triterpene diol, arabidiol, by cytochrome P450 monooxygenase encoded by the root-specific gene *CYP705A1* (Sohrabi et al., 2015). A study using yeast as a model organism has presented the evidence that arabidiol is produced from 2,3-oxidosqualene by the arabidiol synthase PEN1 (Xiang et al., 2006), and the expression of which is synergistically associated with *CYP705A1* (Sohrabi et al., 2015). Nonetheless, the regulation of the key genes in DMNT biosynthesis remains largely unknown.

The *RPX1* gene described in this study encodes for a novel cap-binding protein (nCBP), which is a member of the eukaryotic initiation factor 4E (eIF4E) gene family. In plants, the eIF4E family consists of *eIF4E1*, *eIF4E2*, *eIF(iso)4E* and *nCBP*, which play essential roles in the initiation of cap-dependent mRNA translation (Rhoads, 2009). The eIF4E family members are the primary sources of recessive resistance to potato virus Y (PVY)—the most harmful pathogen affecting potato yield and quality, and the utilisation of CRISPR-Cas9 technology targeting *eIF4E1* gene extends the potato virus Y resistance spectrum of *Solanum tuberosum* (Lucioli et al., 2022). Similarly, CRISPR/Cas9-mediated editing of cassava *eIF4E* isoforms *nCBP-1* and *nCBP-2* reduces the severity and incidence of symptoms caused by cassava brown streak disease (Gomez et al., 2019). Moreover, studies in *Arabidopsis* demonstrate that nCBP deficiency plays a role in limiting the cell-to-cell movement of plant viruses (Keima et al., 2017). Nevertheless, the function of nCBPs in herbivorous defence has not been reported.

Here, we use an integrative approach to functionally characterise the *Arabidopsis* gene *RPX1*, which plays an important role in plant resistance to *P. xylostella*. Our results indicate that the knocking down of *RPX1* results in differentially expressed genes (DEGs) and the accumulation of compounds. One of the upregulated genes is *PEN1*, which is key for DMNT biosynthesis. Infestation of the *rpx1* mutant and DMNT accumulation affect the PM structure of *P. xylostella*, and cause larval developmental defects and death. Further evidence demonstrates that *P. xylostella* infestation and wounding induce RPX1 protein degradation, which may, in turn, lead to plant resistance to insects.

2 | MATERIALS AND METHODS

2.1 | Plant materials and growth conditions

Arabidopsis seeds were ordered from the Nottingham *Arabidopsis* Stock Centre (NASC, http://Arabidopsis.info/). Seeds were surface sterilised, sown on Murashige and Skoog (MS) medium, and stratified at 5°C in a growth chamber under a short-day photoperiod (8 h light, 16 h dark) for 3 days. They were then transferred to 22°C in the greenhouse under a long-day photoperiod (16 h light, 8 h dark) with normal plant maintenance.

2.2 | Choice (preference) and no-choice experiments and bioassays

P. xylostella eggs were purchased from Henan Jiyuan Baiyun Company (Cat: HJB004, developed in 2009, propagated for scientific research in a controlled environment) and incubated in a growth chamber set to 26°C, 16 h light/8 h dark. For choice experiments, we transferred 3-week-old *Arabidopsis* plants (eight wild-type and mutant plants, respectively) into test tanks that were connected to each end of the glass test tube, and the remaining experimental steps were performed as described previously (Chen et al., 2021). The fourth-instar larvae were used and 15 larvae were included in every experimental replicate.

For the no-choice experiment, 3-week-old wild-type and mutant plants were transferred to separate and semi-open petri dishes containing the same number of 15 s-instar *P. xylostella* larvae. The subsequent steps were performed as previously described (Chen et al., 2021).

2.3 | Screening of resistant *Arabidopsis* mutants against *P. xylostella*

We collected 179 T-DNA insertion mutants of *Arabidopsis* for *P. xylostalle* resistance screening. The mutants were grown on MS medium and transplanted into P7 pots (size: 7 × 7 cm) under long-day growth conditions (22°C, 16 h light/8 h dark). To avoid potential environmental influence, we moved and rotated the pots daily. For the initial mutant screening, we set up two replicates by growing each mutant in two pots, with Col-0 plants as a control. After 2 weeks' growth post-transplanting, all the mutants were subjected to preference test of third-instar *P. xylostella* larvae by comparing them with Col-0, as described above. The mutants that showed different larval preference from Col-0 were regarded as candidate resistant or sensitive mutants, and were selected for further experimental validation and functional studies.

2.4 | Plasmid construction and gene transformation

For *RPX1*pro:*RPX1* construct, the *RPX1* genomic coding region with a 1.6 kb of upstream sequence and a 1 kb downstream sequence was PCR-amplified from genomic DNA extracted from Col-0. The assembled DNA fragment was cloned into the pGreenII-0179 vector and transformed into *rpx1-1* mutant using the floral dip method (Clough & Bent, 1998).

To construct *RPX1pro:RPX1-GFP*, *RPX1* promoter (1.6 kb), coding region, and 1 kb 3′ untranslated sequences were PCR-amplified from Col-0 genomic DNA. *GFP* fragment was amplified from a plasmid containing *GFP* sequences. These DNA fragments were assembled into the pGreenII-0179 vector using cut-and-ligation method and then transformed into *rpx1-1* mutant. For *35Spro:RPX1-FLAG* construct, *RPX1* coding sequences were PCR-amplified from cDNA reverse-transcribed from Col-0 mRNA. The PCR fragment was cloned into a pCambia1300-FLAG vector using the infusion method (Clontech) and transformed into Col-0.

35Spro:PEN1, *35Spro:MRN1* (*MARNERAL SYNTHASE 1*) and *35Spro:THAS* (*THALIANA THALIANOL SYNTHASE 1*): The coding sequences of these genes were PCR-amplified from the Col-0 cDNA, and ligated into the pLGNL-35S vector. An artificial microRNA (amiR) targeting *PEN1* was designed as previously described (Schwab et al., 2006), amplified using plasmid pRS300 as a template, and ligated into a modified version of the pCambia1300m vector. All primer sequences are listed in Supporting Information: Table S1.

2.5 | Assays of the activity of glutathione s-transferase (GST) and cytochrome P450 (CYP450) in *P. xylostella* larvae

After the second-instar *P. xylostella* larvae were fed with Col-0 or *rpx1-1* seedlings for 72 h, they were collected and ground to a fine powder in liquid nitrogen. The assays were performed using GST (Nanjing Jiancheng Biology Company, cat: A004) and CYP450 activity analysis kits (Beijing Huabaitai Biology Company, cat: P450), according to the manufacturer's instructions. Each assay had three biological replicates, and each replicate comprised 30 *P. xylostella* larvae.

2.6 | Smurf assays

Three-week-old Col-0 or *rpx1-1* seedlings were used to feed second-instar *P. xylostella* larvae. The assay was performed as previously described with minor modifications (Chen et al., 2021). Six biological replicates were used, and each replicate contained 15 *P. xylostella* larvae.

2.7 | Microscopic observation of PM structure of larvae

Anatomy analysis of larval PM structure and paraffin cross-section analysis of larval intestine was carried out as previously described (Chen et al., 2021).

2.8 | Gene expression analysis and transcriptome sequencing (RNA-seq)

Col-0 and *rpx1-1* seedlings were grown under a long-day growth condition (16 h light, 8 h dark) at 22°C. Two-week-old Col-0 and *rpx1-1* seedlings were used for transcriptome sequencing. Each sample contained three biological replicates. Total RNA was extracted using the RNAprep Pure Plant Kit (TIANGEN, catalogue number: DP441). First-strand cDNAs were synthesised by reverse transcription using the One-Step RT system (Takara Bio) according to the manufacturer's instructions. qRT-PCR was carried out with the gene-specific primers listed in Supporting Information: Table S1 on a Roche Light Cycler 480 instrument. The construction and sequencing of RNA-seq libraries were performed using Biomarker (Beijing, China) on an Illumina HiSeq platform. Finally, we used edgeR to perform differential expression analysis (the threshold of significant difference was set: $|\log2foldchange| \geq 1$, $p < 0.05$). Three biological replicates were performed for Col-0 and *rpx1-1*, and the differentially expressed genes are listed in Data set S1.

2.9 | Extraction and gas chromatography and mass spectrometry (GC-MS) analysis of DMNT and DMNT-^{2}H in *Arabidopsis*

DMNT extraction and analysis were performed as previously described with minor modifications (Sohrabi et al., 2015). In the assays, 2 g of 3-week-old *Arabidopsis* seedlings were used for DMNT extraction and measurement.

2.10 | Preparation and characterisation of DMNT

DMNT was synthesised as previously described, with minor modifications (H. J. Huang & Yang, 2007). Briefly, a 500 ml round-bottomed flask equipped with a Teflon-coated magnetic stirring bar was charged with 1 g (6.48 mmol) of allylic alcohol and 50 ml of dichloromethane. The solution was stirred vigorously and treated with 3.6 g of active manganese dioxide, followed by the addition of 1–2 g of oxidant every 2–3 h until the completion of the reaction. The product was then used to generate the desired compound via a witting reaction. The structure and purity of DMNT were confirmed by ^{1}H nuclear magnetic resonance (NMR) and ^{13}C NMR spectroscopic approaches.

2.11 | DMNT treatment of *P. xylostella*

The assays were performed in petri dishes covered with clear-cling plastic films with multiple holes. DMNT was diluted in paraffin oil (Sigma-Aldrich) to the desired dosage (2.5 nmol/L–25 μmol/L) and injected into the forage as described in the text. All assays were performed in six biological replicates, with each replicate consisting of 15 larvae. Larval growth was recorded by photographic documentation. Forage injected with the same volume of paraffin oil solvent was used as a control.

2.12 | Measurement of JA and SA content in *Arabidopsis* seedlings

The assays were conducted by Nanjing Convinced-test Technology Company. Two-week-old Col-0 and *rpx1-1* seedlings were infested with 15 s-instar *P. xylostella* larvae, with un-infested seedlings as a control. We placed two larvae on each plant of the infestation group to ensure that all plants were infested. After 24 h, plant samples were collected and quickly frozen in liquid nitrogen for JA and SA determination. The samples were grounded to a fine powder in liquid nitrogen and extracted with an isopropanol-water-hydrochloric acid extraction solution, followed by the addition of 8 μl of deuterated salicylic acid (D-SA) and dihydrojasmonic acid (2HJA) (1 μg/ml each) as internal standards. Dichloromethane was then added, and the solution was mixed well on a rotator for 30 min. After the lower organic phase was obtained by centrifugation at 13,000 rpm for 5 min, it was blown dry with nitrogen, re-dissolved in methanol (0.1% formic acid), and then centrifuged at 13,000 g for 10 min. Finally, the supernatant was filtered through a 0.22 μm organic filter membrane and analysed by high-performance liquid chromatography coupled to mass spectrometry (HPLC-MS/MS). All the extraction steps were performed at 4°C. The identities of JA and SA were determined based on the peak time of the target substances and the mass-to-charge ratio (*m/z*) of the corresponding ions. The quantification of JA and SA was fitted using a linear regression equation obtained from internal standard curves. For the acquisition of the internal standard curve, SA and JA standard solutions with gradients of 0.1, 0.2, 0.5, 2, 5, 20, 50 and 200 ng/ml were prepared using methanol (0.1% formic acid) as the solvent, and internal standard solutions with a final concentration of 20 ng/ml were added to the actual plot. The linearity anomalies were removed from the equations of the standard curves. JA: $y = 0.853\ x + 0.00152$ ($r = 0.9958$); SA: $y = 1.76\ x + 0.0403$ ($r = 0.9936$).

2.13 | Analysis of DMNT transportation in *Arabidopsis*

DMNT was dissolved in DMSO and added to MS medium without glucose. Three-week-old *Arabidopsis* plants were transferred to test tubes and their roots were immersed in MS medium with DMNT or DMSO (control). To prevent contamination, the test tubes were covered with two layers of parafilm, and a small hole was made on the film, through which the plant roots were positioned in MS medium for further growth. After 24 h, the roots of the treated plants were removed and their leaves were used to feed *P. xylostella*, and then larval survival and pupation rates were analysed. The same experiment was repeated with growth medium containing either ^{2}H-labelled DMNT or DMSO as a control. After 24 h of incubation, leaves were collected and processed for GC-MS analysis. To rule out the possibility that DMNT may volatilise from DMNT medium to aerial parts and cause tracing contamination, a control group was set up in the same way, but the plant roots were buried with moist cotton and were not immersed in DMNT medium. After 24 h, the aerial parts were harvested for further bioassay or DMNT detection using GC-MS.

2.14 | Protein extraction and immunoblotting analysis of RPX1 in *Arabidopsis* after *P. xylostella* infestation and wounding treatments

We set up two types of treatments on transgenic *RPX1pro:RPX1-GFP* and *35Spro:RPX1-FLAG Arabidopsis* seedlings: *P. xylostella* infestation and wounding. For larval infestation, we grew *Arabidopsis* seedlings for 2 weeks and fed them to second-instar larvae (place at least one larva on each seedling), after 15–120 min, the larvae were removed, and the infested seedlings were selected and harvested for further experiments. To mimic wounding, we used a needle of a 1 ml syringe to create a hole on each *Arabidopsis* leaf. After 15–120 min of growth, the seedlings were collected.

To determine if *P. xylostella* infested plants could induce RPX1 degradation, we infested Col-0 seedlings with *P. xylostella* for 15–120 min and tested its influence on RPX1-GFP in transgenic plants. All the samples were ground to powder in liquid nitrogen, and then equal amounts of infested and noninfested Col-0 were separately mixed with the same amount of RPX1-GFP tissues and incubated in solution at 4°C for 15 min. Finally, the mixture was centrifuged, and the supernatant was subjected to immunoblotting analysis.

For western blot analysis, total proteins were extracted with protein extraction buffer [50 mmol/L Tris-HCl pH8.0, 2.5 mmol/L EDTA pH8.0, 150 mmol/L NaCl, 1/1000 IGPAL (v/v), 10% glycerol (v/v), 7% 2-mercaptoethanol (v/v), 1 mmol/L PMSF and 1×proteinase inhibitor cocktail (Roche)]. The protein extract was then used for PAGE separation and immunoblotting analysis with antibodies against GFP (Roche, dilution: 1/1000) and FLAG (Abcam, dilution: 1/2000). Images were captured using a Tanon 5200 chemiluminescence analysis system.

3 | RESULTS

3.1 | The *Arabidopsis rpx1* mutant has improved resistance to *P. xylostella*

To identify genes involved in *P. xylostella* resistance, we collected 179 *Arabidopsis* mutants and grew them in a controlled greenhouse. Two weeks post-transplantation, we carried out preference test of third-instar *P. xylostella* larvae, in response to each mutant and wild-type Col-0. In this screening experiment, 15 mutants showed different influence on larval preference (data not shown), and one of them was selected for this study and designated as *rpx1-1* (resistance to *P. xylostella*). RPX1 encodes for a novel cap-binding protein (nCBP) (Ruud et al., 1998). The T-DNA insertion mutant was SALK_131503, and the gene expression of *RPX1* was significantly knocked down compared to wild-type Col-0 (Figure 1a, Supporting Information: Figure S1a, Supporting Information: Table S1). When planted nearby, the *rpx1-1* plants showed a significantly lower level of damage by *P.*

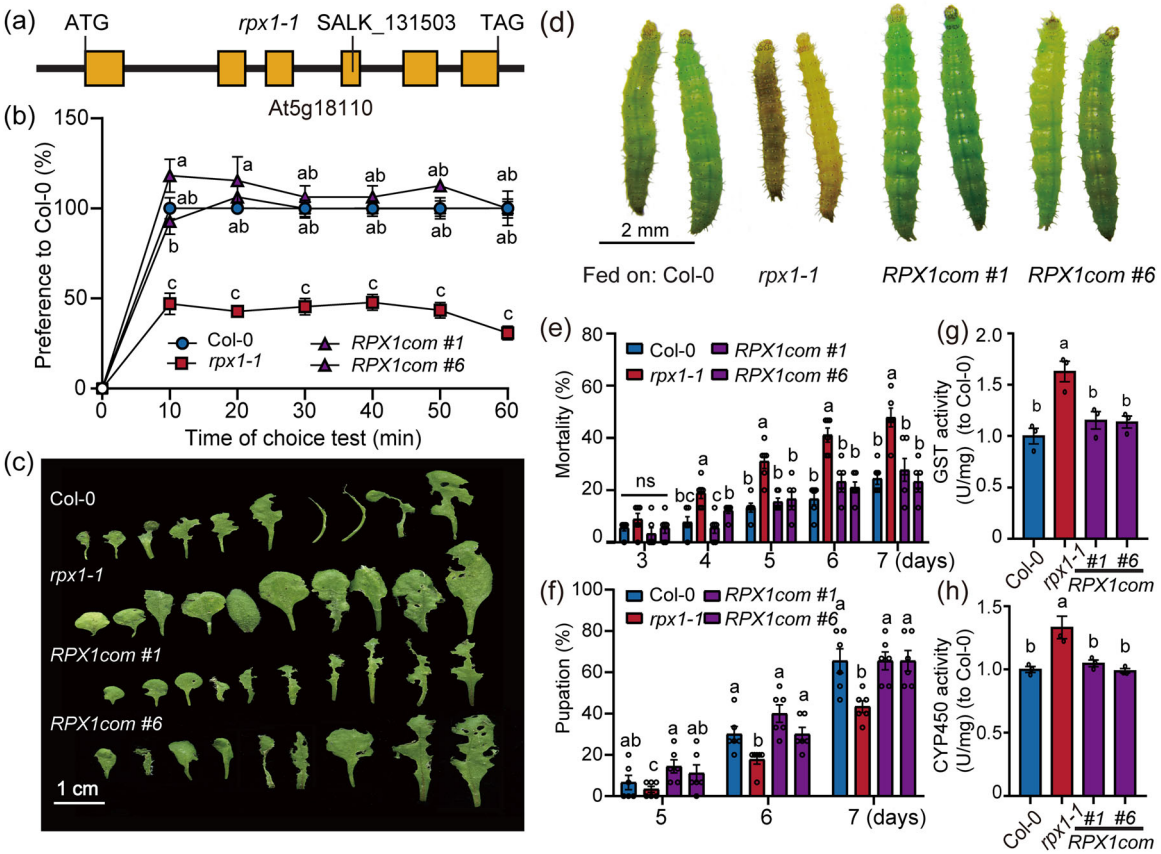

FIGURE 1 Inactivating *RPX1* confers resistance to *Plutella xylostella* in *Arabidopsis*. (a) Gene structure of *RPX1* (At5g18110). Orange boxes indicate exons, and solid lines represent introns and untranslated regions. The T-DNA insertion in SALK_131503, named *rpx1-1*, is on the fourth exon. (b) *P. xylostella* larvae preferentially move toward the wild-type Col-0 and *RPX1* complementation lines (*RPX1pro:RPX1/rpx1-1*, *RPX1com*), compared to *rpx1-1*. (c) Comparison of Col-0, *rpx1-1*, and *RPX1com* leaves infested with *P. xylostella*. (d) *P. xylostella* larvae were severely affected by *rpx1-1*, compared with those on wild-type Col-0 and the *RPX1com* lines, with respect to larval stature, size and colour. (e, f) *P. xylostella* larvae fed with *rpx1-1* show higher mortality (e) and lower pupation (f) rates relative to the wild-type Col-0 and *RPX1com* lines. (g, h) *P. xylostella* larvae fed with *rpx1-1* plants have increased glutathione S-transferase (GST, g) and cytochrome P450 (CYP450, h) activities, whereas in *RPX1com*-fed larvae, the activities showed no difference from those on Col-0. In (b, e–h), data are presented as mean ± s.e.m. The different letters at each treatment indicate a significant difference (one-way analysis of variance, $n = 3$ for b, g, h, $n = 6$ for e, f).

xylostella larvae compared to the wild-type plants (Supporting Information: Figure S1b).

To determine the mechanism underlying *rpx1-1* resistance to *P. xylostella* infestation, we performed preference and no-choice tests. In the preference experiments, *P. xylostella* larvae were placed at the centre of the glass test tube at equal distance from Col-0 and *rpx1-1* seedlings, after 10–60 min, significantly more larvae gathered on the Col-0 side than those on the *rpx1-1* side (Figure 1b). In the no-choice experiments, we fed Col-0 and *rpx1-1* seedlings separately to *P. xylostella* larvae, and observed that Col-0 lost more leaf tissues than the *rpx1-1* mutant (Figure 1c). To confirm that *RPX1* was the causative gene for the observed resistance, we introduced a complementation construct of *RPX1* into the *rpx1-1* mutant. These *RPX1* complementation lines (*RPX1pro:RPX1/rpx1-1*, *RPX1com*) were susceptible to *P. xylostella* infestation, as determined by the preference and no-choice tests (Figure 1b,c), which suggest that *RPX1* is involved in *Arabidopsis* resistance to *P. xylostella*.

3.2 | Growth of *P. xylostella* larvae is negatively affected by the *rpx1-1* mutation

To investigate the physiological response of *P. xylostella* to feeding with *rpx1-1* mutants, we inspected the development of larvae after feeding with 3-week-old plants of Col-0, *rpx1-1* and *RPX1com* lines. The larvae fed with *rpx1-1* plants showed severely compromised development in terms of body size. The body colour of the larvae was also different from that of the larvae fed with Col-0 plants. However, we did not observe such changes in the larvae fed with *RPX1com* seedlings (Figure 1d). Further phenotypic analysis showed that *P. xylostella* larvae fed with *rpx1-1* had markedly higher mortality and lower pupation rates than those fed with Col-0 or *RPX1com* (Figure 1e,f). In addition, larvae fed with *rpx1-1* exhibited higher enzymatic activities of GST and CYP450, which are biomarkers for organ or tissue damage (Cheng et al., 2018; Mikstacki et al., 2015), than those on Col-0 and *RPX1com* (Figure 1g,h), suggesting that the larval tissue might be injured by the feeding of *rpx1-1*.

3.3 | Midgut of *P. xylostella* larvae are damaged after feeding with *rpx1-1* plants

We observed that *rpx1-1*-fed larvae consumed less plant tissues and produced much fewer faeces than those fed with wild-type Col-0; therefore, we hypothesised that the digestion of the larvae fed with *rpx1-1* might be affected. To check if leakage happened in the intestine of the larvae fed with *rpx1-1*, we carried out the 'Smurf test'. The larvae fed with wild-type Col-0 and *RPX1com* lines defecated the dye, and no dye was visually left in the body of the larvae, whereas the *rpx1-1*-fed larvae retained a significant amount of dye in the midgut and the surrounding tissues, and the larvae turned blue (Figure 2a). Quantitative analysis of blue ('Smurf') and normal ('no Smurf') larvae showed that feeding of *rpx1-1* plants resulted in more than three-fold individuals showing 'Smurf' compared to those fed with wild-type Col-0 or *RPX1com* (Figure 2b). These results suggest that feeding of *rpx1-1* is able to cause lesions and higher permeability in the midgut of larvae.

3.4 | Peritrophic matrix of *P. xylostella* is damaged by feeding of *rpx1-1* seedlings

We further dissected and isolated peritrophic matrix (PM) from the larvae fed with Col-0, *rpx1-1* and *RPX1com* seedlings for structural analysis under a stereomicroscope. Compared with the intact and plumb PM of the larvae fed with Col-0 and *RPX1com*, the larvae fed with *rpx1-1* exhibited damage characteristics and were thin, loose and discontinuous (Figure 2c–f). To further confirm the damage characteristics of PM, we obtained transverse sections of the larval samples. Hematoxylin-eosin (HE) staining results revealed that the PM of the larvae fed with Col-0 was thick and intact, and that there was an ectoperitrophic space (ES) between PM and midgut epidermal cells (Figure 2g). In contrast, the PM in the midgut of the larvae fed with *rpx1-1* was severely disrupted, and the intestinal contents were close to the intestinal wall (no es, Figure 2h). When larvae were fed with *RPX1com* seedlings, their PM and es were not significantly altered (Figure 2i,j). These results confirm that *RPX1* knockdown had a negative effect on the PM of *P. xylostella* larvae.

3.5 | Accumulation of DMNT content in the *rpx1-1* confers resistance to *P. xylostella* larvae

To investigate whether knockdown of *RPX1* reshapes the metabolites of *Arabidopsis* and leads to resistance to *P. xylostella* larvae, we compared the volatile organic compounds (VOCs) released from *rpx1-1* and wild-type Col-0 plants. Four VOCs (Hexanol,3-ethyl-5methyl, Octance,2,6-dimethyl, Nonane,2,6-dimethyl and DMNT) were differentially accumulated between *rpx1-1* and Col-0 (Figure 3a).

To further dissect the molecular mechanism of *rpx1-1* in *P. xylostella* resistance, we performed RNA-seq analysis. Compared to Col-0, the *rpx1-1* mutant exhibited 211 differentially expressed genes (DEGs) (Supporting Information: Data Set S1). KEGG enrichment analysis indicated that these DEGs belonged to more than 20 different metabolic pathways, including sesquiterpenoid and triterpenoid biosynthesis, alpha-linolenic acid metabolism, and tyrosine metabolism pathways (Figure 3b, Supporting Information: Table S2). Notably, the most significantly enriched pathway was the biosynthesis of sesquiterpenoids and triterpenoids, which consisted of three DEGs: At4g15340, At5g42600 and At5g48010 (Figure 3b, Supporting Information: Figure S2a–c). At4g15340 has been reported to encode for PEN1, an oxidosqualene cyclase that converts 2,3-oxidosqualene to arabidiol and leads to the synthesis of bioactive DMNT via CYP705A1 (Field & Osbourn, 2008; Sohrabi et al., 2015). At5g42600 encodes for marneral synthase 1 (MRN1), which is a key component in marneral biosynthesis. At5g48010

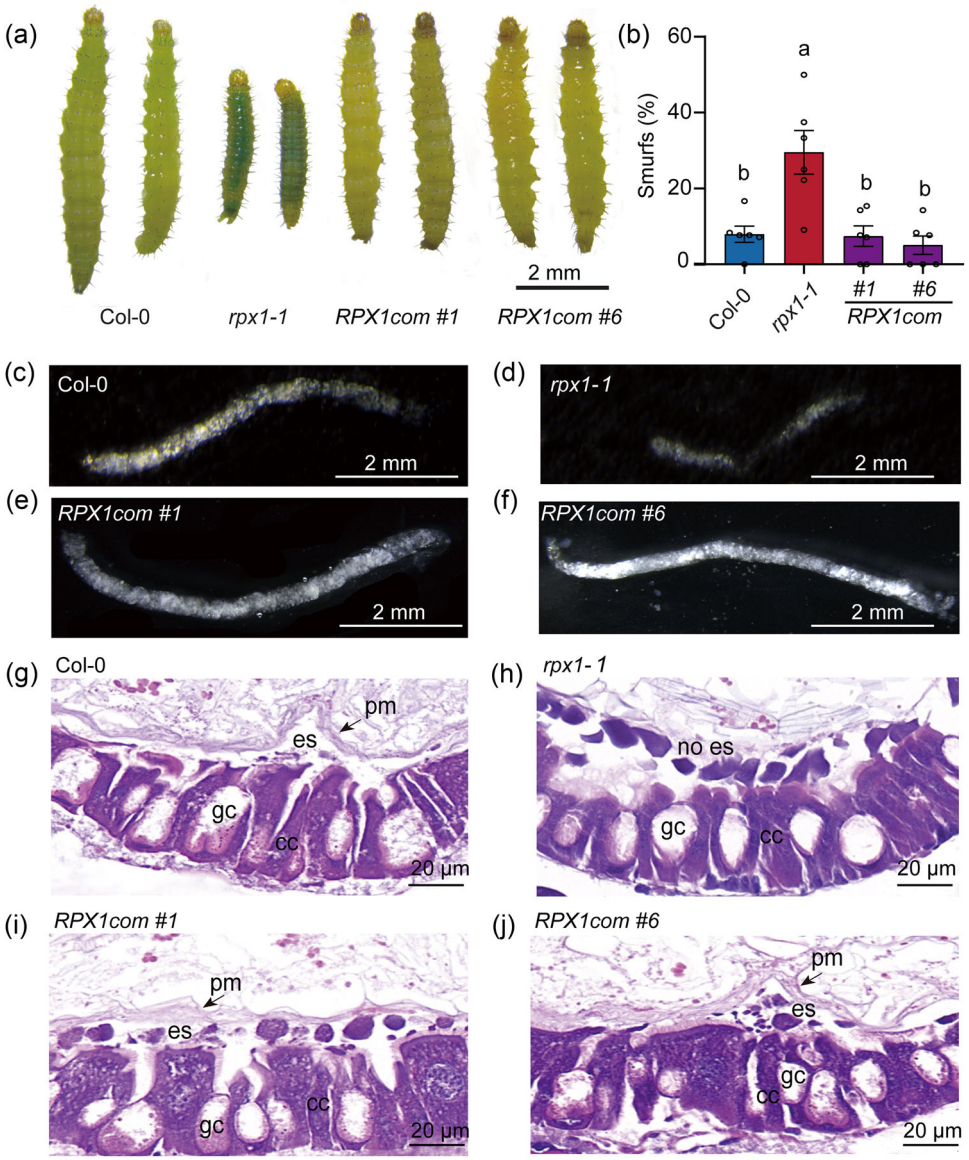

FIGURE 2 RPX1 inactivation damages peritrophic matrix (PM) structure in larval midgut. (a) Representative images of larvae fed with Col-0, *rpx1-1* and *RPX1com* lines showing dye retention, as evidenced by their blue appearance, like the Smurf cartoon character. (b) Quantification of results shown in (a). Data are presented as mean ± s.e.m; the different letters indicate a significant difference (one-way analysis of variance, $n = 6$). (c–f) PM ultrastructure of larvae fed with Col-0 (c), *rpx1-1* (d) and *RPX1com* lines (e, f). Note that the PM of larvae fed with Col-0 and *RPX1com* is plump and intact, but the PM of the larvae fed with *rpx1-1* is thin, delicate, and discontinuous in some regions. (g–j) Transverse section and hematoxylin-eosin staining show damage of the PM from the larvae fed with Col-0 (g), *rpx1-1* (h), or *RPX1com* lines (i, j). [Color figure can be viewed at wileyonlinelibrary.com]

encodes for thalianol synthase (THAS), an enzyme involved in thalianol biosynthesis. Marneral and thalianol have been reported to be involved in the maintenance of plant development (Field & Osbourn, 2008; Go et al., 2012) (Supporting Information: Figure S3). We studied the potential roles of MRN1 and THAS in insect resistance by investigating the preference, mortality and pupation rates of *P. xylostella* by feeding them with the transgenic *Arabidopsis* seedlings overexpressing *MRN1* (*35Spro:MRN1*) and *THAS* (*35Spro:THAS*) (Supporting Information: Figure S4a,b). No significant difference was detected between the two transgenes and the wild-type Col-0 (Supporting Information: Figure S4c–n), suggesting that the insect resistance of *rpx1-1* is not likely dependent on these two genes.

The enrichment of terpenoid biosynthesis in KEGG analysis (Figure 3b) and the differential accumulation of DMNT detected in *rpx1-1* (Figure 3a) suggested that DMNT might be one of the compounds involved in plant resistance to *P. xylostella*. Similar to previous reports that had barely detected DMNT by GC-MS analysis in Col-0 (Liu et al., 2018; Sohrabi et al., 2015), we could detect trace amounts of DMNT in noninfested Col-0 (Figure 4a,b). Whereas in contrast, DMNT levels were highly enriched (~8 ng/g) in *rpx1-1*, and *RPX1com* lines showed very low levels of DMNT, similar to that in

(a)

Peak	RT (min)	Volatile metabolites	Abundance (Col-0)	Abundance (*rpx1-1*)	Significance
1	17.419	Heptane,3-ethyl-5-methyl-	53.3±3.73	67.9 ±5.85	*
2	17.552	Octane,2,6-dimethyl-	26.6±2.05	29.9 ±2.52	*
3	18.808	Nonane,2,6-dimethyl-	24.1±1.13	52.5 ±4.47	*
4	19.307	DMNT	0.19±0.03	15.9 ±1.30	**

(b)

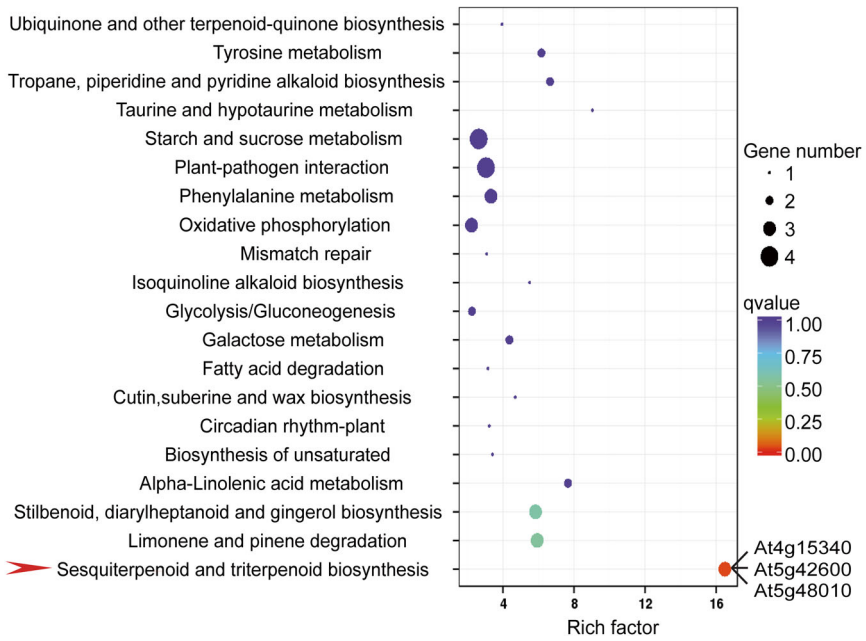

FIGURE 3 Comparison of volatile compounds and gene expression differentially enriched between Col-0 and *rpx1-1*. (a) Differentially enriched volatile compounds in Col-0 and *rpx1-1* were detected by the gas chromatography-mass spectrometry (GC-MS) method. Data are presented as mean ± s.e.m; asterisks indicate a significant difference (*$p < 0.05$, **$p < 0.01$, two-tailed unpaired *t*-test). (b) Transcriptomic analysis of Col-0 and *rpx1-1*. KEGG analysis of pathway enrichment from differently expressed genes between Col-0 and the *rpx1-1* mutant. One enriched pathway (red arrow) is related to sesquiterpenoid and triterpenoid biosynthesis and consists of three genes, as shown in the figure. [Color figure can be viewed at wileyonlinelibrary.com]

Col-0 plants (Figure 4). In addition, upon *P. xylostella* infestation, DMNT levels increased (~20 ng/g) in *rpx1-1*, which was higher than that in the Col-0 and *RPX1com* lines (Figure 4). We synthesised DMNT in vitro using a modified method (Chen et al., 2021). Consistent with previous observations (Chen et al., 2021), DMNT suppressed *P. xylostella* growth, as evidenced by preference (2.5 μmol/L) and no-choice performance (0.25–25 μmol/L) (Supporting Information: Figure S5a,b). Moreover, HE staining results revealed that the PM of control larvae was thick and intact (Supporting Information: Figure S5c), whereas the PM of larvae treated with 2.5 μmol/L DMNT for 48 h was thin and discontinuous in some regions (Supporting Information: Figure S5d). Taken together, our findings suggest that the *rpx1-1* mutation causes DMNT accumulation, which contributes to the killing *of P. xylostella* larvae in *Arabidopsis*.

JA and SA are plant secondary metabolites that are closely related to biotic stress. To determine whether these substances contribute to the insect resistance of *rpx1-1*, we checked the JA and SA levels of Col-0 and *rpx1-1* before and after infestation by *P. xylostella*. Under untreated conditions, there was no significant difference in the levels of JA and SA between *rpx1-1* and Col-0 plants (Supporting Information: Figure S6), and the levels of both hormones increased significantly at 24 h after infestation with *P. xylostella*. Notably, after infestation, the SA content was significantly lower in *rpx1-1* compared with Col-0, whereas the JA content was much higher in *rpx1-1* than that in Col-0 (Supporting Information: Figure S6).

3.6 | RPX1 regulates DMNT accumulation in dependence on PEN1

To investigate the contribution of PEN1 in *rpx1-1* regulated DMNT accumulation, we generated a construct containing an artificial miRNA (*PEN1amiR*) and transformed it into *rpx1-1* mutants. We also generated *a PEN1* overexpression construct, which was transformed into Col-0 (*35pro:PEN1*/Col-0). Gene expression analysis showed that *PEN1* was knocked down (4-7 folds) in *PEN1amiR/rpx1-1* compared with that of *rpx1-1*, and was overexpressed (~2.5 times) in *35Spro:PEN1* compared with Col-0 (Figure 5a). In these transgenic lines, the expression of *RPX1* was not influenced by *PEN1* knockdown

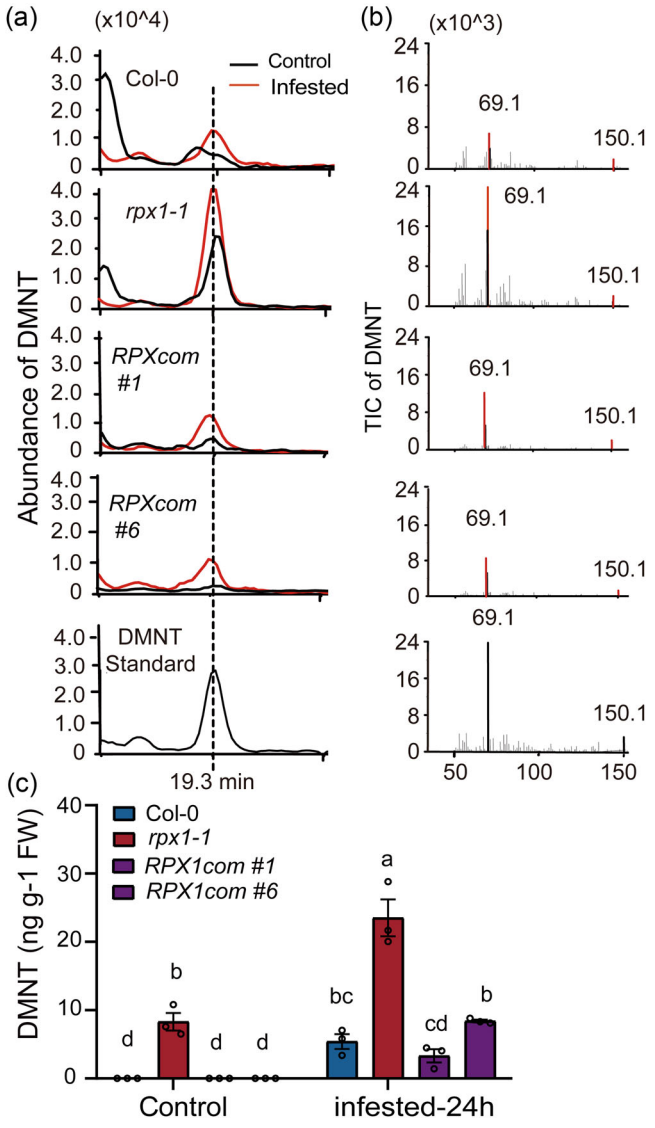

FIGURE 4 Loss of RPX1 increases dimethyl-1,3,7-nonatriene (DMNT) accumulation. (a) gas chromatography-mass spectrometry (GC-MS) analysis of DMNT in Col-0, *rpx1-1* and *RPX1com* (*RPX1pro:RPX1/rpx1-1*) lines. The DMNT standard is shown at the bottom. (b) Total ion chromatography (TIC) of DMNT captured from Col-0, *rpx1-1* and *RPX1com*. (c) DMNT content increases in the *rpx1-1* mutant but returns to wild-type levels in *RPX1com* transgenic plants. Data are presented as mean ± s.e.m; the different letters indicate a significant difference (one-way analysis of variance, $n = 3$). [Color figure can be viewed at wileyonlinelibrary.com]

or overexpression (Figure 5b). When infested with *P. xylostella* for 6-24 h, *PEN1* expression was significantly upregulated in Col-0 and *rpx1-1*, and much higher *PEN1* expression was achieved in *rpx1-1* after 24 h of infestation (Figure 5c). Next, we measured DMNT content in Col-0, *rpx1-1*, *PEN1amiR/rpx1-1* and *35Spro:PEN1*/Col-0. Without *P. xylostella* infestation, *rpx1-1* produced higher levels of DMNT than Col-0 (Figure 5d,e,f,k,l), and when *PEN1* was knocked down by artificial microRNA in *rpx1-1* (*PEN1amiR/rpx1-1*), DMNT levels were downregulated, exhibiting a much lower level than that in *rpx1-1* (Figure 5d,g,h,m,n). Upon larval infestation, the DMNT levels in Col-0 and *rpx1-1* seedlings were significantly upregulated, but in *PEN1amiR/rpx1-1* seedlings, the DMNT level could not be induced and was much lower than that in *rpx1-1* (Figure 5d,g,h,m,n), suggesting that *PEN1* may play an important role in RPX1-regulated DMNT biosynthesis, as illustrated in Supporting Information: Figure S3. Consistent with this, DMNT was highly accumulated in *35Spro:PEN1*/Col-0 seedlings (Figure 5d,i,j,o,p).

3.7 | PEN1 contributes to killing *P. xylostella* in *rpx1-1*

Given the observation that *PEN1* knockdown could attenuate the DMNT accumulation induced by RPX1 inactivation (Figure 5), we performed bioassays on *PEN1* knockdown and overexpression transgenic *Arabidopsis* to demonstrate its biological role. We found that the *P. xylostella* larvae showed no preference for amiR-*PEN1/rpx1-1* plants compared with Col-0 (Supporting Information: Figure S7). Meanwhile, *P. xylostella* larvae fed with *PEN1-amiR/rpx1-1* showed significantly lower mortality and higher pupation rates than *rpx1-1*, whereas the larvae fed with *35Spro:PEN1*/Col-0 showed higher mortality and lower pupation rates than those fed with Col-0 (Figure 6a,b). Consistent with these results, further 'Smurf test' and transection experiments showed that the *PEN1-amiR/rpx1-1* had normal and intact intestines and PM compared to the larvae fed with *rpx1-1* (Figure 6c,d,g,h), and overexpression of *PEN1* caused severe damage to the midgut and PM of *P. xylostella* larvae (Figure 6c,d,i,j). These results suggest that *PEN1* knockdown could suppress the negative effects on larval growth caused by *RPX1* inactivation, thereby playing an important role in *rpx1-1* induced toxic influence on *P. xylostella* larvae.

3.8 | DMNT transports from roots to aerial parts of *Arabidopsis*

PEN1 has been reported to be mainly expressed in *Arabidopsis* roots (A. C. Huang et al., 2019; Sohrabi et al., 2015) (Supporting Information: Figure S8a), which is different from the results that the aerial parts of *rpx1-1* showed toxicity to *P. xylostella* in a PEN1-dependent manner (Figure 6). Therefore, we formulated an alternative hypothesis: plants synthesise DMNT mainly in the roots and transport it to the aerial parts, where it promotes resistance to insects. To test this hypothesis, we performed two DMNT transport assays. In the first assay (Figure 7a), we incubated the roots of 3-week-old *Arabidopsis* seedlings in liquid plant growth medium containing 2.5 µmol/L DMNT, using DMSO as a control. After culturing for 24 h, we excised the *Arabidopsis* leaves and offered them to *P. xylostella* larvae. Compared to the DMSO control, the leaves from DMNT-treated plants caused significantly higher larval mortality and lower pupation rates than the control (Figure 7b,c).

In the second experiment aiming to gain further independent validation of DMNT transport, we labelled DMNT with ^{2}H and added

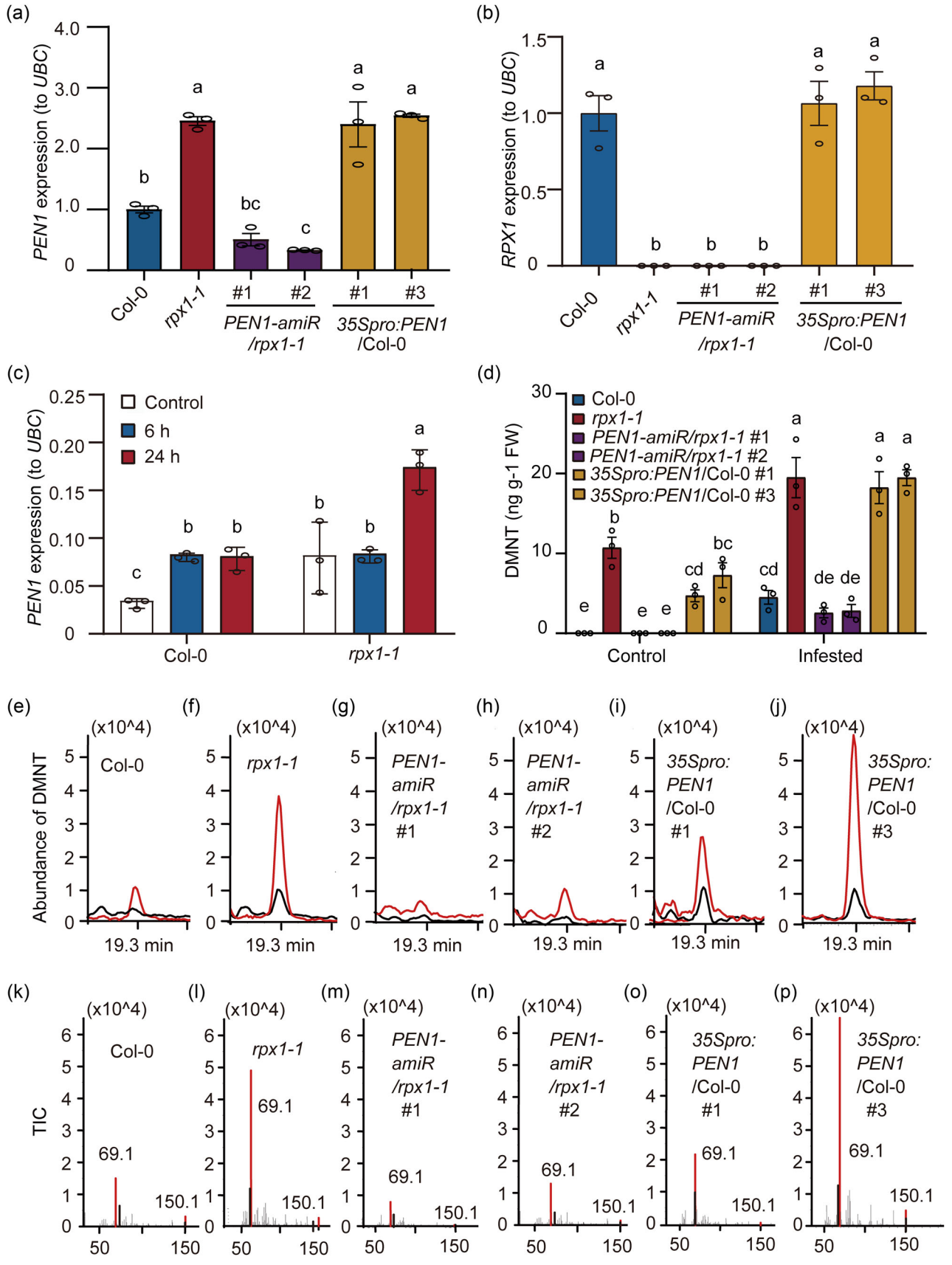

FIGURE 5 (See caption on next page)

DMNT-^{2}H to the liquid plant growth medium. After 24 h of incubation, DMNT-^{2}H was highly enriched in the leaves (Figure 7d–i). To rule out the possibility that DMNT may volatilise from liquid growth medium to the air and contaminate plant aerial parts, we set up a parallel control, which was performed in the same way as in Figure 7a, except that *Arabidopsis* roots were not immersed in liquid growth medium. The results showed that no DMNT-^{2}H was detected in the aerial parts of plants (Supporting Information: Figure S8b,c). Thus, we propose that DMNT moves from the roots, where it is produced, to *Arabidopsis* leaves, where it causes pest death.

3.9 | RPX1 is degraded by *P. xylostella* infestation and wounding treatments

We showed that *PEN1* expression was upregulated in *rpx1-1* and *Arabidopsis* seedlings infested with *P. xylostella* larvae (Figure 5a,c), raising the possibility that RPX1 may also respond to larval infestation. To validate this prediction, we investigated the potential response of *RPX1* to *P. xylostella* infestation. Gene expression analysis showed that *RPX1* was expressed in different tissues (Supporting Information: Figure S9a), but had no significant response to 6–24 h larval infestation (Supporting Information: Figure S9b). Therefore, we checked RPX1 protein levels in *RPX1pro:RPX1-GFP* transgenic plants by performing immunoblotting. The results showed that without larval infestation, RPX1-GFP was stable during 0-120 min; in contrast, after infestation by larvae for 15 min, RPX1-GFP started to degrade; after 120 min, RPX1-GFP protein went continuously down to approximately 6% of the start time point (Figure 8a, Supporting Information: Figure S10a). As a control, in *Arabidopsis* seedlings containing *GFP* transgene, GFP was relatively stable after larval infestation (Figure 8b). To rule out the possible influence of the GFP tag on RPX1 stability, we generated transgenic *RPX1* plants with a FLAG tag (*35Spro:RPX1-FLAG*) to perform larval infestation experiments, which showed consistent results that RPX1-FLAG could also be degraded by larval infestation, similar to RPX1-GFP (Figure 8c).

Insect infestation often causes wounding in plants, and physical damage can partially simulate the feeding process of herbivorous insects. To demonstrate whether wounding could induce RPX1 degradation, we used a needle to create holes in plant leaves to mimic wounding and found that RPX1-GFP degraded after 30 min of treatments (Figure 8d, Supporting Information: Figure S10b). To understand better the reason for RPX1 degradation upon *P. xylostella* infestation, we incubated the tissues of RPX1-GFP transgenic plants together in solution for 15 min with that of Col-0, which had been infested by *P. xylostella* for 15–120 min, or Col-0 tissues without infestation. The immunoblotting analysis showed that RPX1-GFP level from the samples incubated with pre-infested Col-0 was much lower than those with uninfected Col-0 (Figure 8e), suggesting that *P. xylostella* infestation induced some factors or signals in Col-0 that could lead to RPX1 degradation.

3.10 | *rpx1-1* mutation confers an advantage in plant development and reproduction

A common feature of herbivory-specific defence responses is the trade-off between pest resistance and plant growth and reproduction (Li et al., 2018). To determine whether the genotype at the *RPX1* locus is subject to such trade-offs, we compared seed production in Col-0 and *rpx1-1* mutants. In the absence of *P. xylostella* infestation, the seed yield per plant was similar between the two genotypes (Supporting Information: Figure S11). In contrast, exposing 3-week-old *rpx1-1* and Col-0 plants to the infestation of 15 s-instar *P. xylostella* for only 72 h reduced the final seed yield of Col-0 by three folds, whereas the seed yield in *rpx1-1* was not significantly affected. Moreover, the seed yield of *RPX1com* was similar to that of Col-0, but much lower than that of *rpx1-1*, suggesting that RPX1 inactivation confers an advantage in seed production upon larval infestation (Supporting Information: Figure S11). We also assessed seed production in *35Spro:PEN1* transgenic *Arabidopsis* and observed that overexpression of *PEN1* produced a higher seed yield under both larval-infested and un-infested conditions (Supporting Information: Figure S11). These results suggest that the *rpx1-1* mutation and higher *PEN1* expression confer resistance to *P. xylostella* in the absence of a typically associated growth trade-off, highlighting the potential of *RPX1* and *PEN1* in molecular breeding programs aimed at improving crop production.

4 | DISCUSSION

Pests dramatically lower agronomic yields and quality, making plant protection a priority and long-term objective for farmers and breeders. In this study, we identified the *Arabidopsis* mutant *rpx1-1*, which showed high resistance to *P. xylostella*, an important lepidopteran pest of crops. Our analysis revealed that *rpx1-1* mutation resulted in higher *PEN1* transcript levels, DMNT accumulation, and improved plant resistance against pests. We also showed that RPX1 protein could be degraded by larval infestation and wounding treatment.

FIGURE 5 PEN1 contributes an important role in dimethyl-1,3,7-nonatriene (DMNT) accumulation in *rpx1-1*. (a) *PEN1* expression analysis in Col-0, *rpx1-1*, *PEN1* knockdown in *rpx1-1* background (*PEN1-amiR/rpx1-1*) and *PEN1* overexpression (*35Spro:PEN1*/Col-0) lines. (b) *RPX1* expression in Col-0, *rpx1-1*, *PEN1-amiR/rpx1-1* and *35Spro:PEN1*/Col-0. (c) *PEN1* expression is induced by *Plutella xylostella* infestation in Col-0 and *rpx1-1*. (d) Comparison of DMNT accumulation between Col-0, *rpx1-1*, *PEN1-amiR/rpx1-1* and *35Spro:PEN1*/Col-0. (e–j) gas chromatography-mass spectrometry (GC-MS) analysis of volatiles emitted from Col-0 (e), *rpx1-1* (f), *PEN1-amiR/rpx1-1* (g, h) and *35Spro:PEN1*/Col-0 (i, j) lines. (k–p) TIC of DMNT captured from Col-0 (k), *rpx1-1* (l), *PEN1-amiR/rpx1-1* (m, n) and *35Spro:PEN1*/Col-0 (o, p) lines, corresponding to the data in (e–j). In (a–d), data are presented as mean ± s.e.m; the different letters indicate a significant difference (one-way analysis of variance, $n = 3$). [Color figure can be viewed at wileyonlinelibrary.com]

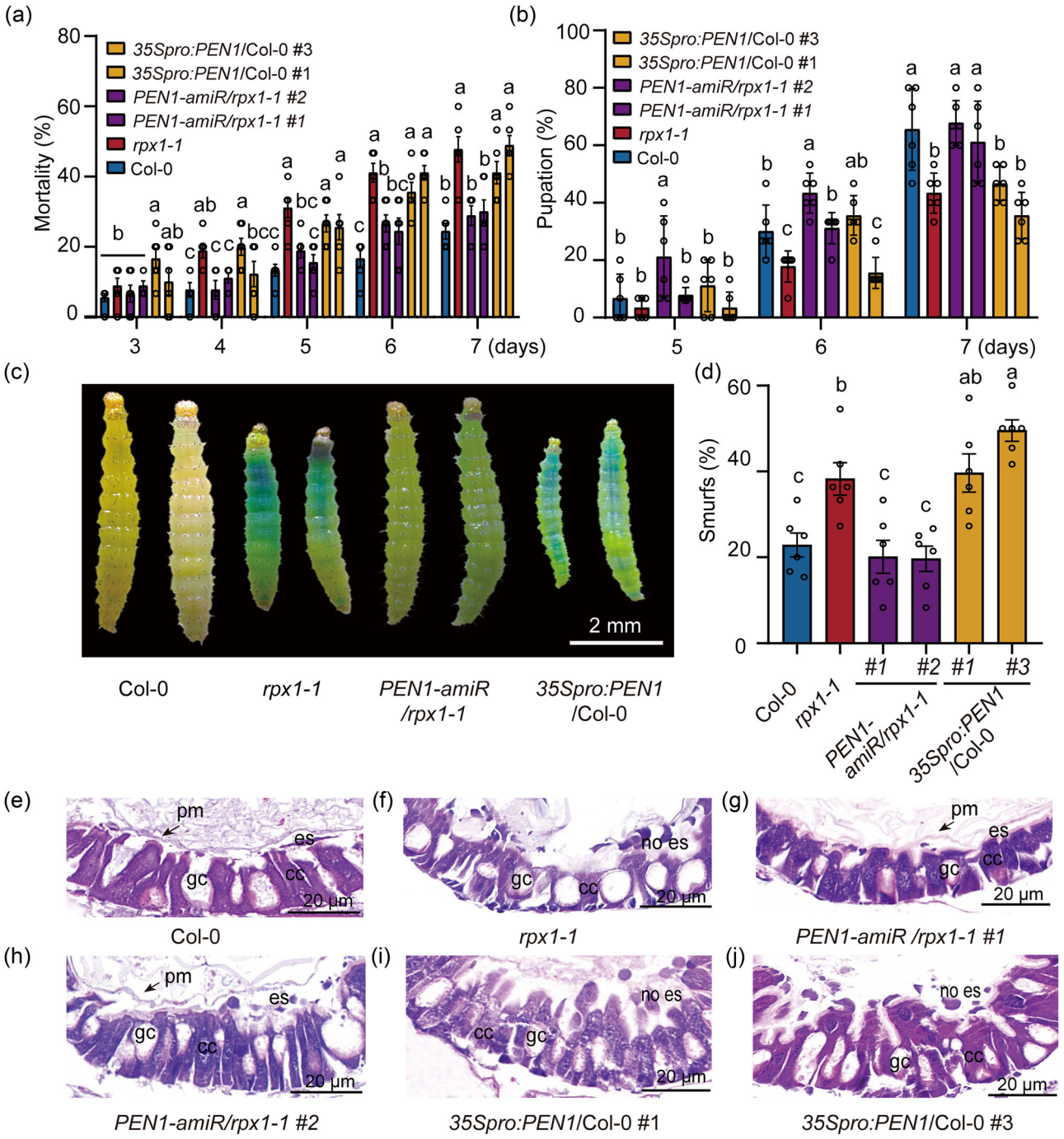

FIGURE 6 PEN1 contributes to the enhanced resistance of *rpx1-1* to *Plutella xylostella*. (a, b) *PEN1-amiR* transgene significantly alleviates the resistance of *rpx1-1* to *P. xylostella* infestation, while *35Spro:PEN1* enhances the resistance effect, as demonstrated by mortality (a) and pupation (b) rates of *P. xylostella* larvae. (c) Representative images of the larvae fed with Col-0, *rpx1-1*, *PEN1-amiR/rpx1-1* and *35Spro:PEN1* seedlings showing dye retention, as evidenced by their blue appearance, like the Smurf cartoon character. (d) Quantification results of images shown in (c). (e–j) Transverse section and hematoxylin-eosin staining show damage of the PM from the larvae fed with Col-0 (e), *rpx1-1* (f), *PEN1-amiR/rpx1-1* (g, h) and *35Spro:PEN1* seedlings (i, j). Data are presented as mean ± s.e.m; the different letters at each treatment indicate a significant difference in (a, b, d) (one-way analysis of variance, $n = 6$). [Color figure can be viewed at wileyonlinelibrary.com]

In the no-choice tests, the *rpx1-1* mutant exhibited significant resistance to *P. xylostella* infestation (Figure 1c). Conversely, *P. xylostella* larvae fed with *rpx1-1* plants showed severe negative developmental afflictions (Figure 1d,e). These phenotypes are attributable to the inactivation of RPX1, because *RPX1* complementation lines (*RPX1com*) are as susceptible as the wild-type Col-0 (Figure 1c–e), supporting the conclusion that RPX1 is involved in pest resistance. In addition to killing larvae, the *rpx1-1* mutant also had a long-term effect on larval development, including pupation (Figure 1f), leading to reduced reproduction of the pest.

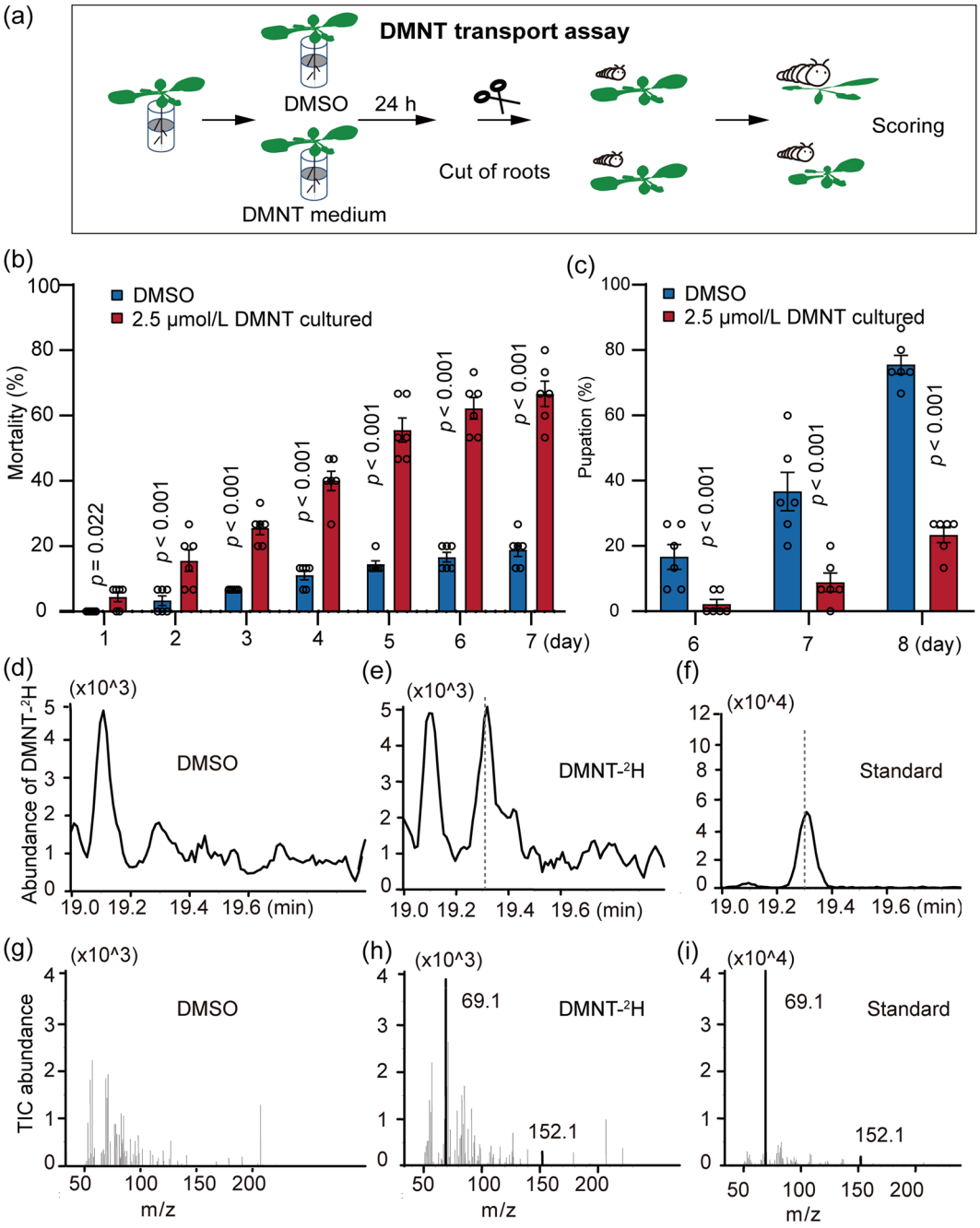

FIGURE 7 Dimethyl-1,3,7-nonatriene (DMNT) transports from *Arabidopsis* roots to leaves. (a) Illustration of the DMNT transport assay using *Arabidopsis* seedlings. DMNT was dissolved in Murashige and Skoog liquid medium. After 24-h culture, the roots were excised, and the leaves were used to feed *Plutella xylostella* larvae for mortality and pupation rate scoring. (b, c) DMNT, transported from roots to leaves, results in higher mortality (b) and lower pupation (c) rates of *P. xylostella* larvae. (d–f) ^{2}H-labelled DMNT (DMNT-^{2}H) is transported from root to leaves. DMNT-^{2}H was dissolved in liquid MS medium as in (a) for 24 h, and then the leaves were harvested for GC-MS analysis (e). DMSO was used as a control (d). DMNT-^{2}H standard is shown for reference (f). (g–i) TIC of DMNT-^{2}H obtained during the transport assays shown in (d–f). Data are presented as mean ± s.e.m, in (b, c) $n = 6$, *p*-values are shown adjacent to the histogram columns to indicate a significant difference (two-tailed unpaired *t*-test). Note that more controls for the transport assays are included in Supporting Information: Figure S8. [Color figure can be viewed at wileyonlinelibrary.com]

Furthermore, preference tests indicated that the wild-type Col-0 and *rpx1-1* mutants might emit different volatile compounds; one of them is DMNT, which is effective in repelling pests (Figures 1b, 3a, Supporting Information: Figure S5a). Based on the above results, we propose that DMNT accumulation in *rpx1-1* is one of the reasons for insect poisoning. JA and SA signalling pathways have been reported to be involved in insect resistance (Costarelli et al., 2020; Lortzing & Steppuhn, 2016). In this study, after 24 h of insect feeding, the content of JA and SA in both Col-0 and *rpx1-1* mutants increased, and the increase in SA content in *rpx1-1* was significantly lower than that

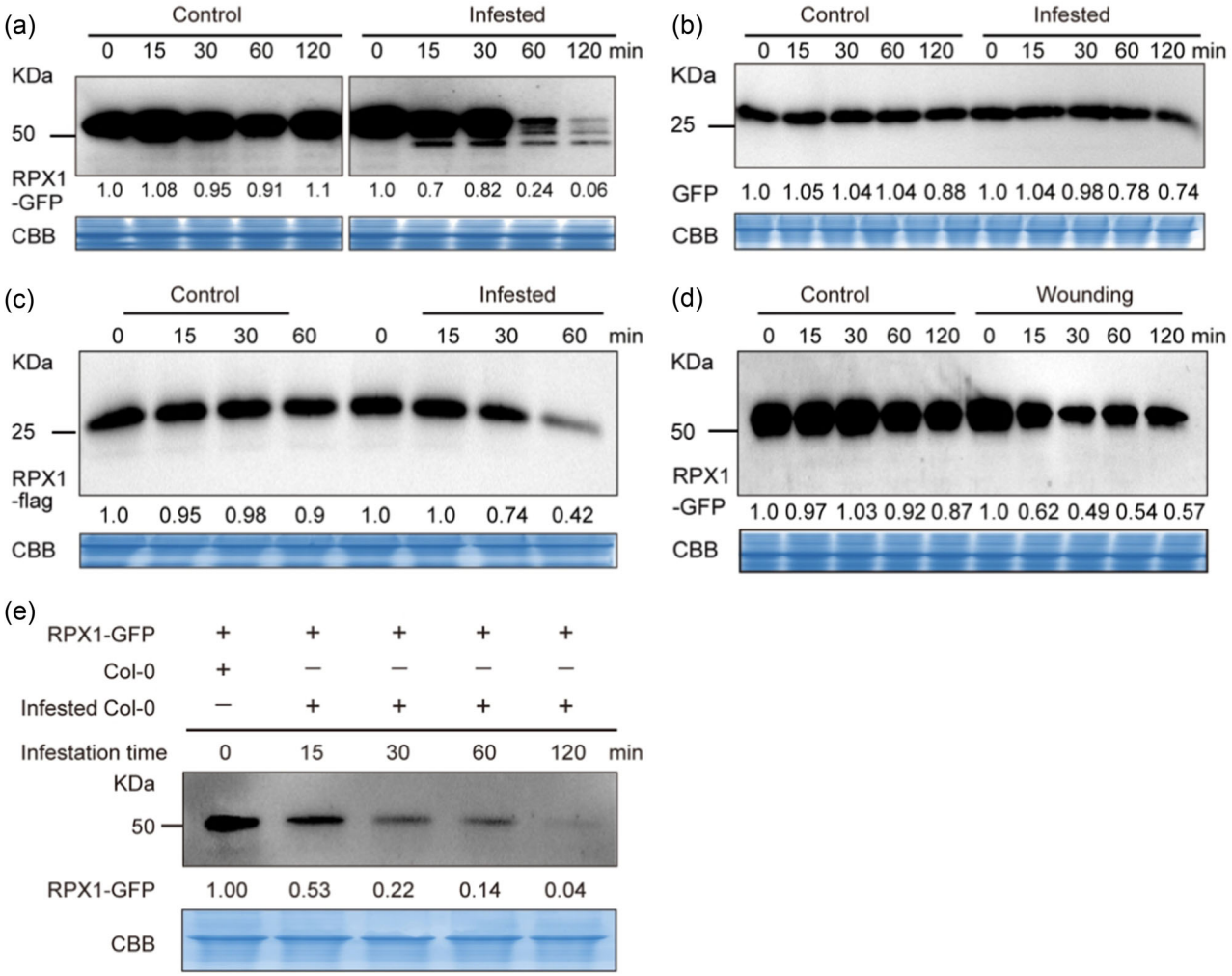

FIGURE 8 RPX1 protein degradation is induced by *Plutella xylostella* infestation, wounding treatments. (a) RPX1-GFP from *RPX1pro:RPX1-GFP* transgenic plants are degraded upon *P. xylostella* infestation for 15−120 min. (b) As a control for (a), GFP itself from *35Spro:GFP* transgenic plants show no degradation upon larval infestation. (c) *RPX1-flag* from *35Spro:RPX1-flag* transgenic plants are degraded upon larval infestation. (d) RPX1-GFP from *RPX1pro:RPX1-GFP* transgenic plants are degraded by 15−120 min of wounding treatment. (e) RPX1-GFP from *RPX1pro:RPX1-GFP* transgenic plants are degraded when the tissues are incubated in solution with the tissues from Col-0 plants that have been infested by *P. xylostella* for 15−120 min. The values below immune-blotting bands show the relative protein abundance quantified using ImageJ. All these experiments have been repeated at least three times, and representative results are shown. More experimental data with independent transgenic lines are shown in Supporting Information: Figure S10. [Color figure can be viewed at wileyonlinelibrary.com]

in Col-0, while the increase in JA content was much higher (Supporting Information: Figure S6), suggesting that JA and SA may also play important roles in the *rpx1-1*'s resistance to *P. xylostella*. Therefore, we propose that both direct and indirect effects of *rpx1-1* contribute to enhanced resistance of *Arabidopsis* against insects.

We present several lines of evidence demonstrating how PEN1-mediated DMNT accumulation contributes to RPX1 functions in plant resistance to *P. xylostella*. *PEN1*, a key gene belonging to sesquiterpenoid and triterpenoid biosynthesis pathway, was identified from the KEGG analysis of RNA-seq data from *rpx1-1* mutant (Figure 3b), providing a link between RPX1, PEN1 and DMNT (Sohrabi et al., 2015). In support of DMNT as one of the causative compounds that kill pest larvae, DMNT accumulated higher in *rpx1-1* mutants than in Col-0 (Figure 3a), but the level in *RPX1com* lines was reversed to Col-0 (Figure 4a–c). In addition, chemically synthesised DMNT could repel and kill *P. xylostella* larvae (Supporting Information: Figure S5a,b), which is in line with the results of the *rpx1-1* (Figure 1b,e). Furthermore, transgenic plants overexpressing *PEN1* produced more than four times of the DMNT in Col-0 and conferred similar resistance to *P. xylostella* as the *rpx1-1* (Figures 5d,i,j,o,p and 6). Importantly, reducing *PEN1* transcript levels in the *rpx1-1* blocks DMNT biosynthesis (Figure 5d,g,h,m,n) and alleviates the killing effect on *P. xylostella* larvae, which are susceptible to *P. xylostella* infestation (Figure 6a,b). These combined results indicate that the *PEN1* mutation can suppress the function of RPX1 inactivation in pest resistance. RPX1 lesion causes higher *PEN1* abundance (Figure 5a), nevertheless how exactly RPX1 regulates PEN1 and mediates DMNT biosynthesis needs further studies. Since

RPX1 is predicted as a novel cap-binding protein belonging to eIF4E family (Rhoads, 2009; Ruud et al., 1998), it's possible that RPX1 may affect *PEN1* by influencing its mRNA stability or protein translation efficiency, which will be an important topic in future study. Moreover, it should be noted that DMNT levels could still be induced to a higher level by *P. xylostella* infestation in the *rpx1-1* mutant (Figure 5d), suggesting that there may be some other pathways regulating DMNT accumulation independent of RPX1.

DMNT has been detected in a wide range of plant species, such as *Arabidopsis* (Sohrabi et al., 2015), cotton (Liu et al., 2018) and maize (Richter et al., 2016). In addition, it confers indirect protection against herbivore pests by attracting predators, allowing plants to remove pest threats (Kappers et al., 2005; Lee et al., 2010; Li et al., 2018). We recently reported that it could repel and kill *P. xylostella* larvae by damaging the PM in the larval midgut (Chen et al., 2021). Here, we found that the PM structure could be severely damaged when the larvae were fed with *rpx1-1* or *PEN1* over-expressing seedlings (Figures 2c–j and 6i,j). These results are in line with the finding in the DMNT treatment experiments we described previously (Chen et al., 2021), again supporting the proposal that DMNT accumulation in *rpx1-1* may be one of the factors contributing to pest repulsion and death. *RPX1* belongs to the eIF4E gene family (Rhoads, 2009) and is involved in the cell-to-cell movement of plant viruses (Keima et al., 2017). However, whether DMNT accumulation links to viral resistance in plants remains unclear.

PEN1 is specifically expressed in *Arabidopsis* roots, where it catalyzes DMNT biosynthesis (Sohrabi et al., 2015). Consistently in this study, we detected high *PEN1* expression in the roots and very low expression in the leaves (Supporting Information: Figure S8a). We observed that the leaves of the *rpx1-1* mutant were toxic to *P. xylostella* larvae (Figure 1), suggesting that the accumulation of DMNT and the associated pest resistance in leaves cannot be simply explained by minute *PEN1* expression in these tissues. Meaningfully, we found that DMNT could be transported from plant roots to aerial parts, as shown by DMNT transport assays and GC-MS analysis of leaf extracts from the plants incubated with DMNT-^{2}H at their roots (Figure 7). How this compound is transported within plants is unclear, and it may be a topic for further investigation.

Plants have the ability to tolerate and fight against insect attacks in various ways. Here, by performing immunoblotting analysis of *RPX1pro:RPX1-GFP* and *35Spro:RPX1-FLAG* transgenic plants, we found that upon *P. xylostella* infestation, RPX1 protein could be degraded quickly (Figure 8a,c, Supporting Information: Figure S10a), whereas, at the mRNA expression level, *RPX1* remained unaffected (Supporting Information: Figure S9b). Currently, how RPX1 protein is degraded remains unclear, but our data have primarily suggested that the protein degradation mechanism may be involved in the signalling pathways of wounding (Figure 8d, Supporting Information: Figure S10b). Moreover, *P. xylostella* pre-infested Col-0 induced RPX1-GFP degradation in different plants (Figure 8e), suggesting that *P. xylostella* infestation may cause an accumulation of signals in plants that could, in turn, lead to RPX1 degradation. It will be interesting to figure out the identity of the signals in the future. This characteristic of RPX1 degradation is important for plants, which may lead to DMNT accumulation and provide a quick response to pest damage (Supporting Information: Figure S3).

Increased plant tolerance to pests often comes at the expense of fitness. The observation that the *rpx1-1* mutation leads to enhanced resistance (Figure 1) and higher seed production (Supporting Information: Figure S11) in *Arabidopsis* without significant trade-offs offers a promising avenue for engineering crops with higher pest resistance. For example, genome editing via CRISPR-Cas9 is a powerful tool for crop improvement (Yang et al., 2017) that allows the introduction of mutations in *RPX1* and potentially expands its applications to various crops.

ACKNOWLEDGEMENTS

We thank Dr. Xiongyuan Si from the Anhui Agricultural University for technical advice on the DMNT assay in *Arabidopsis*. This work was supported by the Anhui Provincial Major Science and Technology Project (202203a06020005) and the National Natural Science Foundation of China (32171954).

CONFLICT OF INTEREST

The authors declare no conflict of interest.

DATA AVAILABILITY STATEMENT

All data are available in the main text or supporting information. RNA deep sequencing (RNA-seq) data were submitted to the Gene Expression Omnibus (GEO) database of the National Centre for Biotechnology Information (NCBI) (accession code: GSE161940).

ORCID

Peijin Li http://orcid.org/0000-0003-1579-7553

REFERENCES

Arimura, G., Ozawa, R., Shimoda, T., Nishioka, T., Boland, W. & Takabayashi, J. (2000) Herbivory-induced volatiles elicit defence genes in Lima bean leaves. *Nature*, 406, 512–515.

Chen, C., Chen, H., Huang, S., Jiang, T., Wang, C., Tao, Z. et al. (2021) Volatile DMNT directly protects plants against *Plutella xylostella* by disrupting the peritrophic matrix barrier in insect midgut. *eLife*, 10, e63938.

Cheng, X., Hu, J., Li, J., Chen, J., Wang, H., Mao, T. et al. (2018) The silk gland damage and the transcriptional response to detoxifying enzymes-related genes of *Bombyx mori* under phoxim exposure. *Chemosphere*, 209, 964–971.

Clough, S.J. & Bent, A.F. (1998) Floral dip: a simplified method for Agrobacterium-mediated transformation of *Arabidopsis thaliana*. *The Plant Journal*, 16, 735–743.

Costarelli, A., Bianchet, C., Ederli, L., Salerno, G., Piersanti, S., Rebora, M. et al. (2020) Salicylic acid induced by herbivore feeding antagonizes jasmonic acid mediated plant defenses against insect attack. *Plant Signaling & Behavior*, 15, e1704517.

Douglas, A.E. (2018) Strategies for enhanced crop resistance to insect pests. *Annual review of plant biology*, 69, 637–660.

Feng, Y. & Zhang, A. (2017) A floral fragrance, methyl benzoate, is an efficient green pesticide. *Scientific Reports*, 7, 42168.

Field, B. & Osbourn, A.E. (2008) Metabolic diversification—independent assembly of operon-like gene clusters in different plants. *Science*, 320, 543–547.

Go, Y.S., Lee, S.B., Kim, H.J., Kim, J., Park, H.Y., Kim, J.K. et al. (2012) Identification of marneral synthase, which is critical for growth and development in *Arabidopsis*. *The Plant Journal*, 72, 791–804.

Gols, R. (2014) Direct and indirect chemical defences against insects in a multitrophic framework. *Plant, Cell & Environment*, 37, 1741–1752.

Gomez, M.A., Lin, Z.D., Moll, T., Chauhan, R.D., Hayden, L., Renninger, K. et al. (2019) Simultaneous CRISPR/Cas9-mediated editing of cassava eIF4E isoforms nCBP-1 and nCBP-2 reduces cassava brown streak disease symptom severity and incidence. *Plant Biotechnology Journal*, 17, 421–434.

Gouinguené, S., Pickett, J.A., Wadhams, L.J., Birkett, M.A. & Turlings, T.C.J. (2005) Antennal electrophysiological responses of three parasitic wasps to caterpillar-induced volatiles from maize (*Zea mays* mays), cotton (*Gossypium herbaceum*), and cowpea (*Vigna unguiculata*). *Journal of Chemical Ecology*, 31, 1023–1038.

Handrick, V., Robert, C.A.M., Ahern, K.R., Zhou, S., Machado, R.A.R., Maag, D. et al. (2016) Biosynthesis of 8-O-methylated benzoxazinoid defense compounds in maize. *The Plant Cell*, 28, 1682-1700.

Huang, A.C., Jiang, T., Liu, Y.X., Bai, Y.C., Reed, J., Qu, B. et al. (2019) A specialized metabolic network selectively modulates *Arabidopsis* root microbiota. *Science*, 364, eaau6389.

Huang, H.J. & Yang, W.B. (2007) Synthesis of moenocinol and its analogs using BT-sulfone in Julia-Kocienski olefination. *Tetrahedron Letters*, 48, 1429–1433.

Jing, T., Du, W., Gao, T., Wu, Y., Zhang, N., Zhao, M. et al. (2020) Herbivore-induced DMNT catalyzed by CYP82D47 plays an important role in the induction of JA-dependent herbivore resistance of neighboring tea plants. *Plant, Cell & Environment*, 44, 1178–1191.

Johnson, S.N. & Züst, T. (2018) Climate change and insect pests: resistance is not futile? *Trends in Plant Science*, 23, 367–369.

Jouzani, G.S., Valijanian, E. & Sharafi, R. (2017) *Bacillus thuringiensis*: a successful insecticide with new environmental features and tidings. *Applied Microbiology and Biotechnology*, 101, 2691–2711.

Kappers, I.F., Aharoni, A., van Herpen, T.W.J.M., Luckerhoff, L.L.P., Dicke, M. & Bouwmeester, H.J. (2005) Genetic engineering of terpenoid metabolism attracts bodyguards to *Arabidopsis*. *Science*, 309, 2070–2072.

Keima, T., Hagiwara-Komoda, Y., Hashimoto, M., Neriya, Y., Koinuma, H., Iwabuchi, N. et al. (2017) Deficiency of the eIF4E isoform nCBP limits the cell-to-cell movement of a plant virus encoding triple-gene-block proteins in *Arabidopsis thaliana*. *Scientific Reports*, 7, 39678.

Lee, S., Badieyan, S., Bevan, D.R., Herde, M., Gatz, C. & Tholl, D. (2010) Herbivore-induced and floral homoterpene volatiles are biosynthesized by a single P450 enzyme (CYP82G1) in *Arabidopsis*. *Proceedings of the National Academy of Sciences*, 107, 21205–21210.

Li, B., Förster, C., Robert, C.A.M., Züst, T., Hu, L., Machado, R.A.R. et al. (2018) Convergent evolution of a metabolic switch between aphid and caterpillar resistance in cereals. *Science Advances*, 4, eaat6797.

Liu, D., Huang, X., Jing, W., An, X., Zhang, Q., Zhang, H. et al. (2018) Identification and functional analysis of two P450 enzymes of *Gossypium hirsutum* involved in DMNT and TMTT biosynthesis. *Plant Biotechnology Journal*, 16, 581–590.

Lortzing, T. & Steppuhn, A. (2016) Jasmonate signalling in plants shapes plant-insect interaction ecology. *Current Opinion in Insect Science*, 14, 32–39.

Lu, H., Luo, T., Fu, H., Wang, L., Tan, Y., Huang, J. et al. (2018) Resistance of rice to insect pests mediated by suppression of serotonin biosynthesis. *Nature Plants*, 4, 338–344.

Lucioli, A., Tavazza, R., Baima, S., Fatyol, K., Burgyan, J. & Tavazza, M. (2022) CRISPR-Cas9 targeting of the eIF4E1 gene extends the potato virus Y resistance spectrum of the *Solanum tuberosum* L. cv. desirée. *Frontiers in Microbiology*, 13, 873930.

Ma, F., Yang, X., Shi, Z. & Miao, X. (2019) Novel crosstalk between ethylene- and jasmonic acid-pathway responses to a piercing-sucking insect in rice. *New Phytologist*, 225, 474–487.

Meents, A.K., Chen, S.P., Reichelt, M., Lu, H.H., Bartram, S., Yeh, K.W. et al. (2019) Volatile DMNT systemically induces jasmonate-independent direct anti-herbivore defense in leaves of sweet potato (*Ipomoea batatas*) plants. *Scientific Reports*, 9, 17431.

Mikstacki, A., Zakerska-Banaszak, O., Skrzypczak-Zielinska, M., Tamowicz, B., Szalata, M. & Slomski, R. (2015) Glutathione S-transferase as a toxicity indicator in general anesthesia: genetics and biochemical function. *Journal of Clinical Anesthesia*, 27, 73–79.

Rhoads, R.E. (2009) eIF4E: new family members, new binding partners, new roles. *Journal of Biological Chemistry*, 284, 16711–16715.

Richter, A., Schaff, C., Zhang, Z., Lipka, A.E., Tian, F., Köllner, T.G. et al. (2016) Characterization of biosynthetic pathways for the production of the volatile homoterpenes DMNT and TMTT in *Zea mays*. *The Plant Cell*, 28, 2651–2665.

Ruud, K.A., Kuhlow, C., Goss, D.J. & Browning, K.S. (1998) Identification and characterization of a novel cap-binding protein from *Arabidopsis thaliana*. *Journal of Biological Chemistry*, 273, 10325–10330.

Schwab, R., Ossowski, S., Riester, M., Warthmann, N. & Weigel, D. (2006) Highly specific gene silencing by artificial microRNAs in *Arabidopsis*. *The Plant Cell*, 18, 1121–1133.

Shakeel, M., Farooq, M., Nasim, W., Akram, W., Khan, F.Z.A., Jaleel, W. et al. (2017) Environment polluting conventional chemical control compared to an environmentally friendly IPM approach for control of diamondback moth, *Plutella xylostella* (L.), in China: a review. *Environmental Science and Pollution Research*, 24, 14537–14550.

Sohrabi, R., Huh, J.H., Badieyan, S., Rakotondraibe, L.H., Kliebenstein, D.J., Sobrado, P. et al. (2015) In planta variation of volatile biosynthesis: an alternative biosynthetic route to the formation of the pathogen-induced volatile homoterpene DMNT via triterpene degradation in *Arabidopsis* roots. *The Plant Cell*, 27, 874–890.

Varsani, S., Grover, S., Zhou, S., Koch, K.G., Huang, P.C., Kolomiets, M.V. et al. (2019) 12-oxo-phytodienoic acid acts as a regulator of maize defense against corn leaf aphid. *Plant Physiology*, 179, 1402–1415.

Wu, X.M., Yang, C.Q., Mao, Y.B., Wang, L.J., Shangguan, X.X. & Chen, X.Y. (2016) Targeting insect mitochondrial complex I for plant protection. *Plant Biotechnology Journal*, 14, 1925–1935.

Xiang, T., Shibuya, M., Katsube, Y., Tsutsumi, T., Otsuka, M., Zhang, H. et al. (2006) A new triterpene synthase from *Arabidopsis thaliana* produces a tricyclic triterpene with two hydroxyl groups. *Organic Letters*, 8, 2835–2838.

Yang, N., Wang, R. & Zhao, Y. (2017) Revolutionize genetic studies and crop improvement with high-throughput and genome-scale CRISPR/Cas9 gene editing technology. *Molecular Plant*, 10, 1141–1143.

Zhao, Y., Huang, J., Wang, Z., Jing, S., Wang, Y., Ouyang, Y. et al. (2016) Allelic diversity in an NLR gene BPH9 enables rice to combat planthopper variation. *Proceedings of the National Academy of Sciences*, 113, 12850–12855.

Zhou, S. & Jander, G. (2021) Engineering insect resistance using plant specialized metabolites. *Current Opinion in Biotechnology*, 70, 115–121.

SUPPORTING INFORMATION

Additional supporting information can be found online in the Supporting Information section at the end of this article.

How to cite this article: Chen, H., Chen, C., Huang, S., Zhao, M., Wang, T., Jiang, T. et al. (2023) Inactivation of RPX1 in *Arabidopsis* confers resistance to *Plutella xylostella* through the accumulation of the homoterpene DMNT. *Plant, Cell & Environment*, 46, 946–961. https://doi.org/10.1111/pce.14528